CONF-830103--39

RELATIONSHIP OF CORE EXIT-TEMPERATURE NOISE TO THERMAL-HYDRAULIC CONDITIONS IN PWRs[1]

F. J. Sweeney
Oak Ridge National Laboratory
Oak Ridge, Tennessee

B. R. Upadhyaya
The University of Tennessee
Knoxville, Tennessee
and
Analysis and Measurement Services
Knoxville, Tennessee

CONF-830103--39

DE83 006144

---

[1] Research sponsored by the Office of Nuclear Regulatory Research, U.S. Nuclear Regulatory Commission under Interagency Agreement 40-551-75 with the U.S. Department of Energy under contract W-7405-eng-26 with the Union Carbide Corporation.

ACKNOWLEDGEMENTS

The authors thank J. C. Robinson, Technology for Energy Corp., for his valuable observations and suggestions concerning temperature noise in PWRs and the LOFT staff for their technical assistance in performing the noise measurements.

ABSTRACT

Core exit thermocouple temperature noise and neutron detector noise measurements were performed at the Loss of Fluid Test Facility (LOFT) reactor and a Westinghouse, 1148 MW(e) PWR to relate temperature noise to core thermal-hydraulic conditions. The noise analysis results show that the RMS of the temperature noise increases linearly with increasing core ΔT at LOFT and the commercial PWR. Out-of-core test loop temperature noise has shown similar behavior.

The phase angle between core exit temperature noise and in-core or ex-core neutron noise is directly related to the core coolant flow velocity. However, if the thermocouple response time is slow, compared to the coolant transit time between the sensors, velocities inferred from the phase angle are lower than measured coolant flow velocities.

Our results indicate that core exit temperature noise is a potentially valuable tool for the detection of thermal-hydraulic anomalies such as flow blockages or boiling.

NOMENCLATURE

C_p	specific heat capacity of the coolant
δ	fluctuating quantity

Δ	difference operator
$E\{\}$	expectation operator
f	frequency (Hz)
$G(j\omega)$	transit delay transfer function including sensor response
j	$\sqrt{-1}$
$\dot{m}$	mass flow rate
θ	phase angle (deg)
τ	time delay (sec)
T_O	outlet temperature
T_I	inlet temperature
$X(k)$	kth sample of time series X
ω	frequency (rad/s)
Q	power

INTRODUCTION

Temperature signals contain both steady-state (dc) and random fluctuating components (noise). Temperature noise has been studied extensively in out-of-pile sodium (1-3) and water test loops (4,5) as a means of detecting boiling, blockages, and abnormal power skews. However, few experiments have been reported in which core exit temperature noise measurements have been performed in operating pressurized water reactors (PWRs). This lack of knowledge about the behavior of core exit temperature noise hampered the assessment of core damage and sensor failure by noise analysts after the Three Mile Island accident (6). The purpose of the work reported here was to characterize the behavior of core exit temperature noise and its relationship to thermal-hydraulic conditions in PWRs during normal operation. Possible sources and behavior of core exit temperature noise were studied via physical and empirical stochastic models.

MEASUREMENT AND ANALYSIS PROCEDURE

Core exit thermocouple temperature and neutron detector noise measurements were performed at a Westinghouse, 1148 MW(e) PWR and at the Loss of Fluid Test Facility (LOFT) reactor (a 50 MW(th), 1/55 scale model of a commercial PWR). The neutron detector and thermocouple locations for LOFT and the PWR are shown in Figs. 1 and 2 respectively. The dc component of the thermocouple and neutron signals were removed by using a coupling capacitor; the resulting noise signals were amplified (with a gain of 50,000 to 100,000 for the thermocouple signal), recorded on magnetic tape, and reduced via an off-line digital Fourier analyzer as shown in Fig. 3. Single signals were displayed in the frequency domain as real-valued power spectral densities (PSDs) and pairs of signals displayed as complex-valued (represented as magnitude and phase) cross-power spectral densities (CPSDs). The root mean square (RMS)

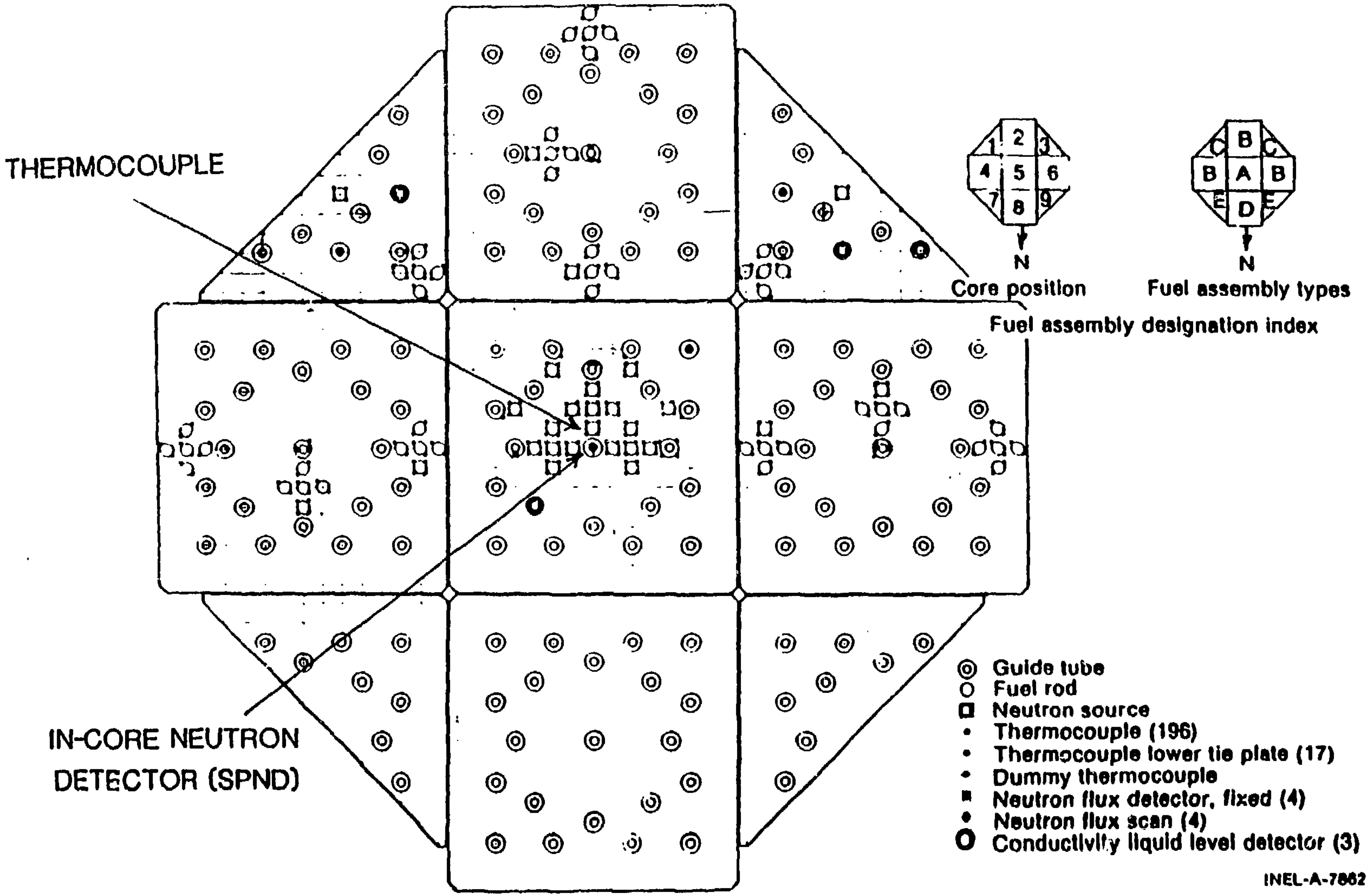

Fig. 1. Location of in-core self powered neutron detector (SPND) and core exit thermocouple at LOFT.

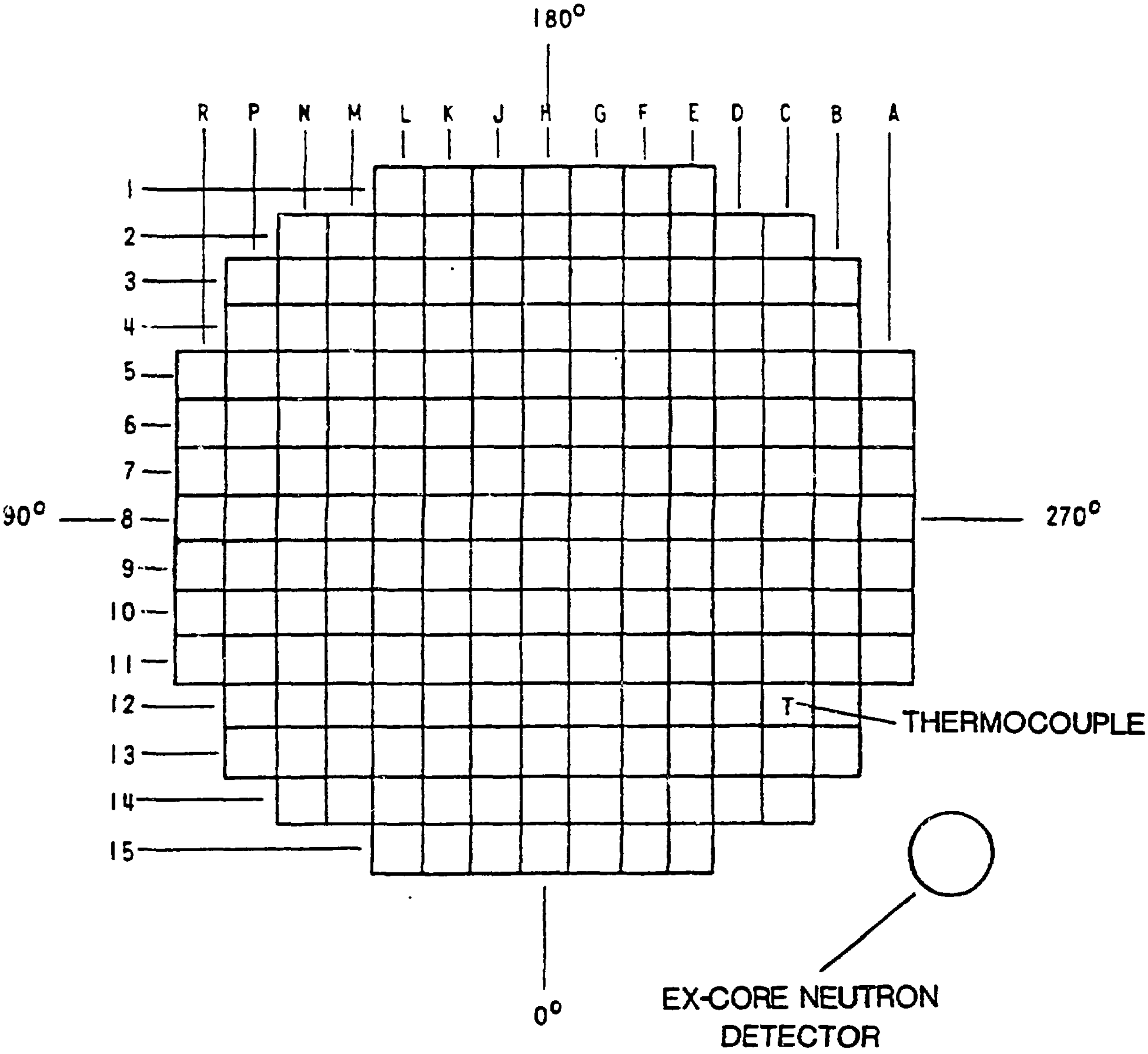

Fig. 2. Location of ex-core neutron detector and core exit thermocouple at the commercial PWR.

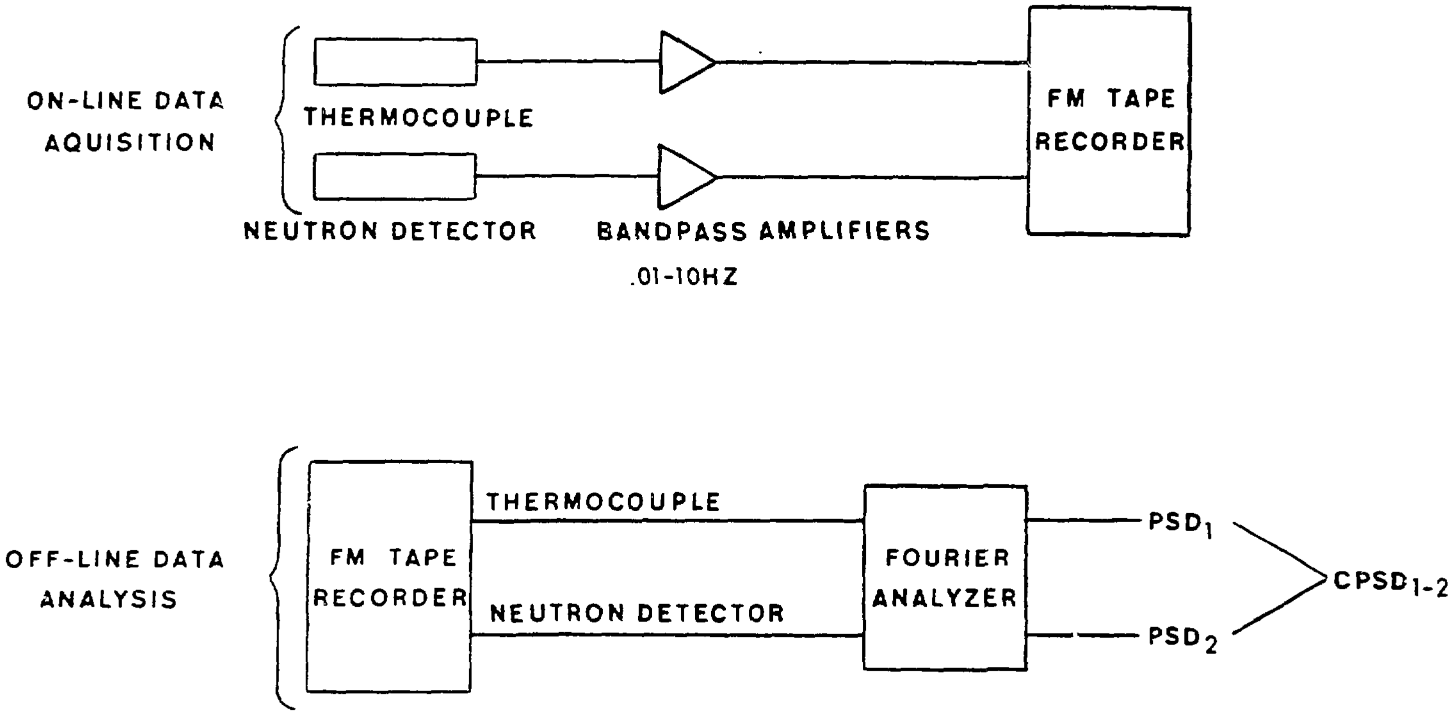

Fig. 3. Noise analysis process used at LOFT and the commercial PWR.

of a signal was obtained from the following formula:

$$\mathrm{RMS} = \left\{ \int_{f_1}^{f_2} \mathrm{PSD}(f)\, df \right\}^{1/2} , \qquad (1)$$

which is the square root of the area under the PSD curve between the frequency limits f_1 and f_2.

RELATIONSHIP OF RMS TEMPERATURE NOISE TO CORE ΔT

The RMS of thermocouple temperature noise has been shown to be a sensitive indicator of flow blockages, boiling, and abnormal power skews in out-of-core fuel assembly test loops (4). In those tests, the RMS temperature noise of a fuel assembly exit thermocouple increased linearly with increasing temperature rise (ΔT) across the assembly, but when blockages or abnormal power skews occurred, the RMS deviated from the original linear behavior.

We performed noise measurements at the commercial PWR and LOFT under varying power levels and flow rates (therefore different core ΔTs) in order to determine whether the core exit RMS temperature noise is also a linear function of core ΔT in PWRs under normal operation. Figure 4 shows that the RMS temperature noise (over the frequency range from 0.1 to 1.0 Hz) is a linear function of core ΔT for the commercial PWR.

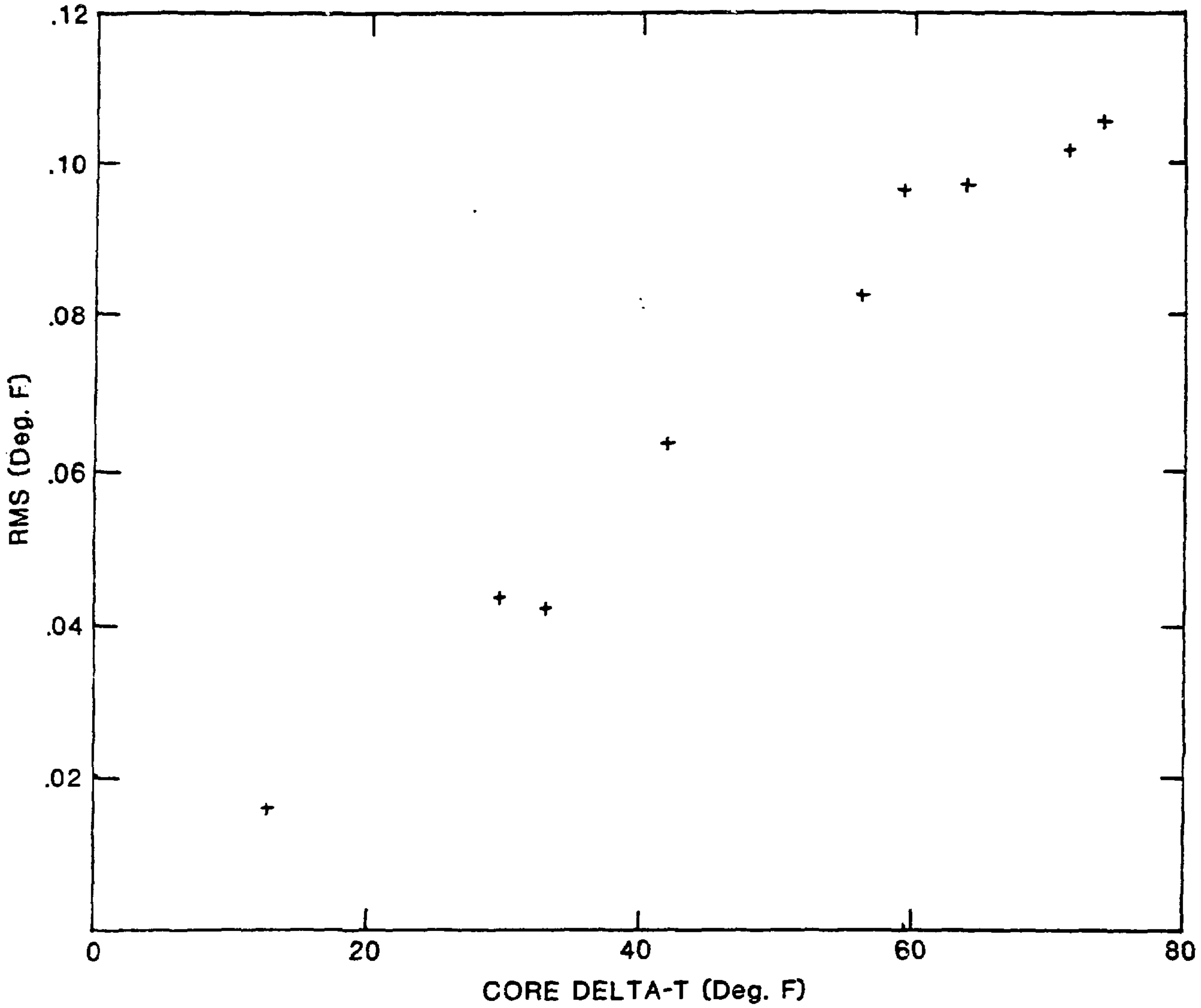

Fig. 4. Core exit temperature noise RMS vs core ΔT at a commercial PWR.

The data for Fig. 4 encompass a range of 2.8 to 100% of rated power at constant flow rate.

The RMS temperature noise for the LOFT reactor is also a linear function of core ΔT, as shown in Fig. 5. The LOFT data include power levels of 27 to 100% of rated power and 65 to 100% of full rated flow. Over these ranges of operating conditions the RMS temperature noise vs core ΔT curve is independent of the coolant flow rate.

A comparison of Fig. 4 with Fig. 5 shows that for a given core ΔT the RMS temperature noise is approximately three times greater for LOFT than for the commercial PWR. The greater RMS values at LOFT may be attributed to the smaller, 2.54 cm (1 in.) distance of the thermocouple from the fuel assembly exit vs the 30.48 cm (12 in.) distance at the commercial PWR. Such dependence of the temperature noise RMS on the separation distance has been observed in out-of-core test loops (5). Differences in turbulence and sensor response time between LOFT and the commercial PWR may also cause the observed differences in RMS temperature noise.

Figures 4 and 5 also indicate that as the core ΔT approaches zero the RMS temperature noise also approaches zero. A single-node model of temperature noise was developed to help understand this phenomenon.

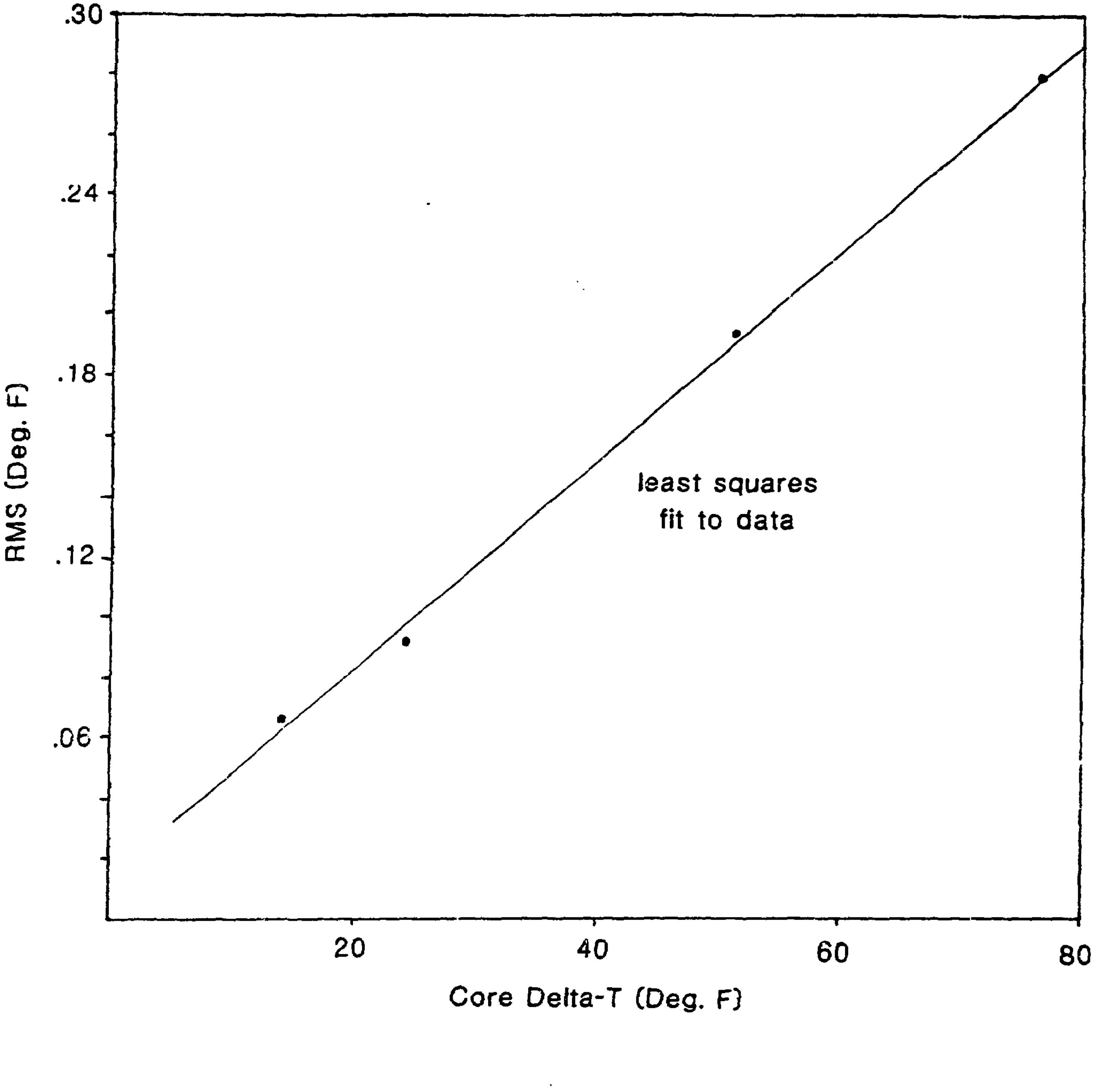

Fig. 5. Core exit temperature noise RMS vs core ΔT at the LOFT reactor.

SINGLE NODE MODEL OF TEMPERATURE NOISE

The reactor was assumed to be represented as a single node, which is described by the following equations:

$$Q = \dot{m}C_p \; (T_O - T_I) \; , \qquad (2)$$

$$\overline{Q} = \overline{\dot{m}}C_p \; (\overline{T}_O - \overline{T}_I) \; , \qquad (3)$$

and assuming only fluctuations in $\dot{m}$, T_O, and T_I,

$$\dot{m} = \overline{\dot{m}} + \delta\dot{m} \; , \qquad (4)$$

$$T_O = \overline{T}_O + \delta T_O \; , \qquad (5)$$

$$T_I = \overline{T}_I + \delta T_I \; , \qquad (6)$$

where the barred symbols represent mean values and the δ symbols represent fluctuating components.

In order to obtain a relationship between the outlet temperature fluctuations and the other variables, Eq. (4-6) are substituted in Eq. (2), and Eq. (3) is subtracted from the result. Linearizing and solving for δT_O yields

$$\delta T_0 = \delta T_I - \frac{\delta m}{\dot{m}} (T_0 - T_I) \; . \qquad (7)$$

$\delta \dot{m}$ and δT_I are assumed to be stochastic (random) variables; therefore, a statistical descriptor such as RMS is needed to describe the relationship between δT_0, δT_I, and δm. The RMS is calculated by squaring Eq. (7), applying the expectation operator, and taking the square root of the result

$$\mathrm{RMS} = \sqrt{E\left\{\delta T_0^{\,2}\right\}} = \sqrt{E\left\{\left[\delta T_I - \frac{\delta \dot{m}}{\dot{m}} (\bar{T}_0 - \bar{T}_I)\right]^2\right\}} \; . \qquad (8)$$

If one assumes $\delta \dot{m}$ and δT_I are statistically uncorrelated, Eq. (8) yields

$$\mathrm{RMS}\ (\delta T_0) = \sqrt{E\left\{\left[\frac{\delta \dot{m}}{\dot{m}} \left(\bar{T}_0 - \bar{T}\right)\right]^2\right\} + E\left\{\delta T_I^{\,2}\right\}} \; . \qquad (9)$$

Equation (9) indicates that inlet, core-coolant temperature fluctuations will produce a core exit RMS temperature noise vs core ΔT curve that does not pass through zero. The assumption that $\delta \dot{m}$ and δT_I are statistically uncorrelated also leads to a core exit RMS temperature noise vs core ΔT curve that is non-linear if the inlet temperature fluctuations are significant.

A multi-nodal model of heat transfer dynamics was also developed (7). Preliminary results from this model indicate that core-inlet temperature fluctuations contribute less than 5% to the core-exit temperature noise.

Based on these results, we conclude that core inlet temperature fluctuations contribute a negligible amount to the core exit temperature noise.

COOLANT VELOCITY MEASUREMENT USING TEMPERATURE/NEUTRON NOISE CROSS CORRELATION

When CPSDs are calculated between core exit thermocouple temperature noise and in-core or ex-core neutron detector noise in PWRs, linear phase angles vs frequency have been observed (8,9). A linear behavior of the phase angle vs frequency indicates a time delay process between the neutron flux and the core exit temperature noise.

To study the relationship between the time delay inferred from this phase angle and core coolant flow velocities, core exit thermocouple and neutron detector noise were simultaneously recorded at both the LOFT reactor and at the commercial PWR. In-core, self-powered neutron detector (SPND) noise at LOFT and ex-core ionization chamber noise at the commercial PWR were cross correlated (CPSDs calculated) with core exit thermocouple temperature noise. Time delays were inferred from a least squares fit of the slope of the phase angle vs frequency plots over the frequency range from 0.05 to 2.0 Hz using the relationship

$$\tau = \frac{\Delta\theta}{360 \cdot \Delta f} \quad . \tag{10}$$

The time delays inferred from the phase vs frequency plots shown in Fig. 6 and the 119.4 cm (47 in.) distance from the SPND to the core exit thermocouple were used to experimentally infer coolant velocities for two different flow rates at LOFT. These experimentally inferred values were compared with velocities calculated from LOFT flow venturi measurements; the results are summarized in Table 1.

The excellent agreement between the velocities inferred from noise analysis and the calculated velocities indicates that the neutron-flux to temperature-noise phase is an indicator of coolant flow velocity in the core.

In a similar manner, time delays and velocities were inferred at a commercial PWR from the phase between an ex-core ionization chamber and the core exit thermocouple noise shown in Fig. 7. The inferred coolant flow velocity was 3.02 m/s (9.90 ft/s); ~37% lower than the calculated 4.82 m/s (15.80 ft/s) for an

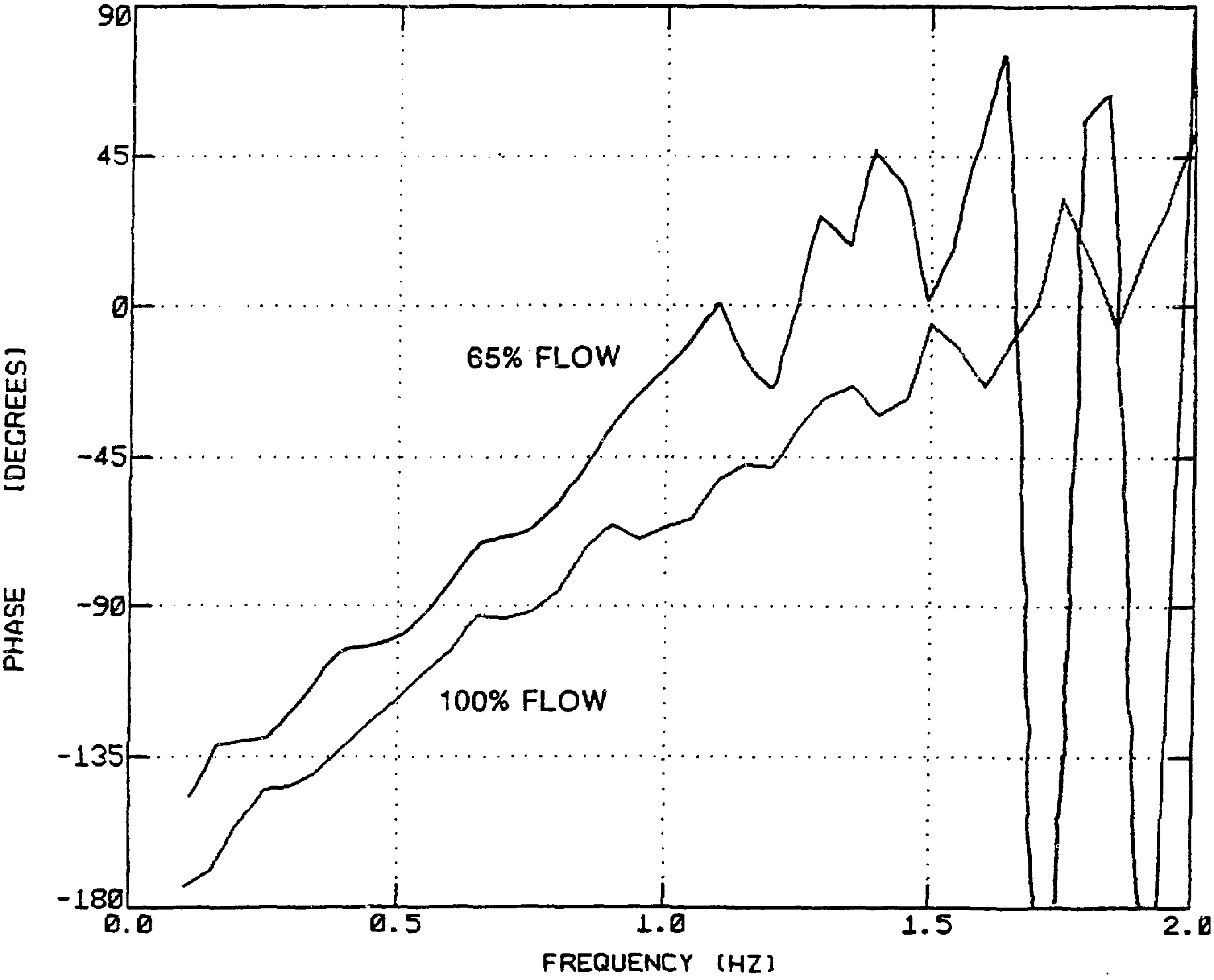

Fig. 6. Linear phase vs frequency between core exit temperature and in-core neutron noise at LOFT for two flow rates.

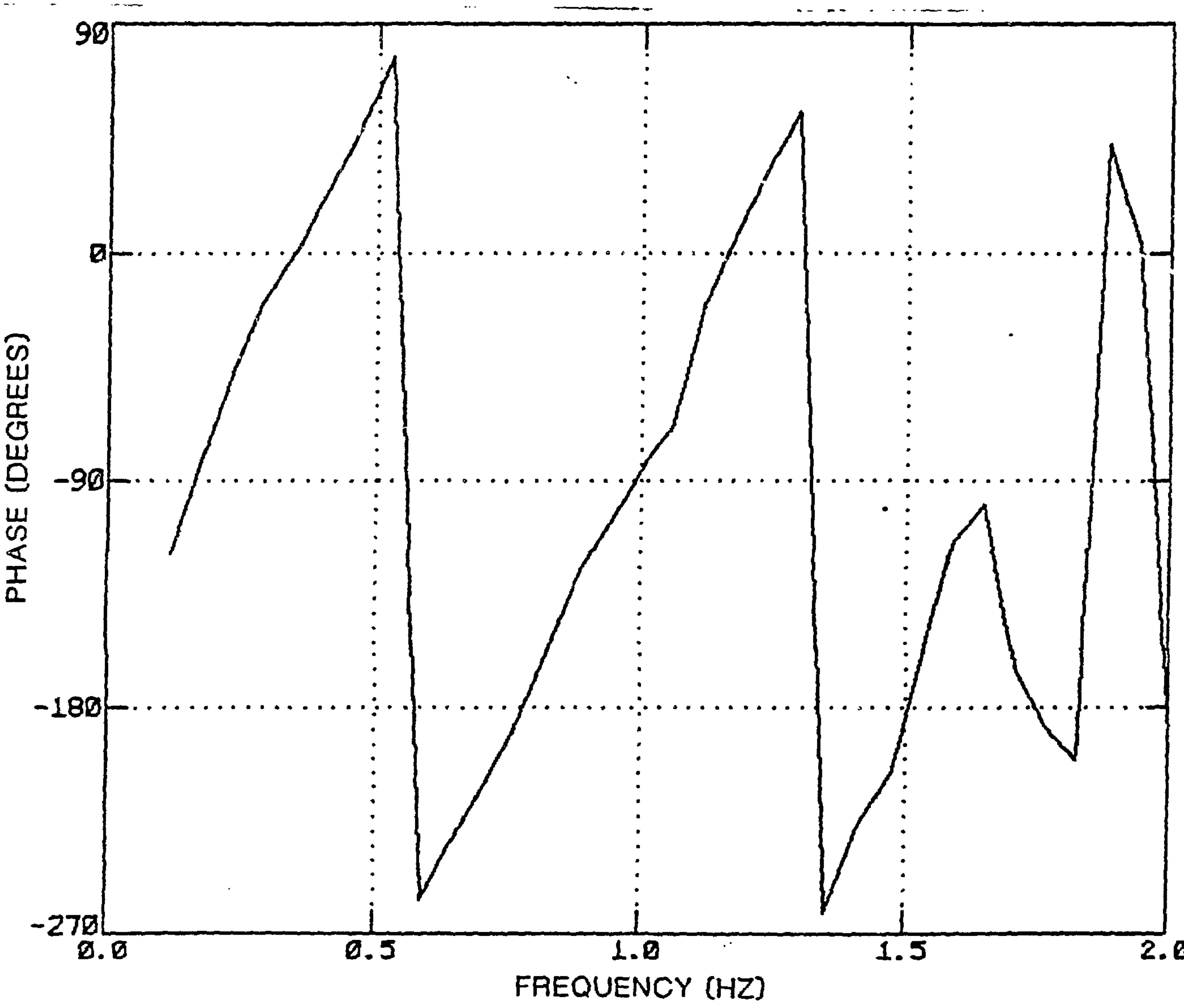

Fig. 7. Linear phase vs frequency between core exit temperature and ex-core neutron noise at a commercial PWR.

assumed distance of 304.8 cm (120 in.) between the ionization chamber midplane and the thermocouple location. A similar discrepancy between velocities inferred from ex-core neutron and core-exit temperature noise has also been observed in other PWRs (9).

EFFECT OF THERMOCOUPLE TIME RESPONSE ON INFERRED COOLANT VELOCITIES

We studied the effects of thermocouple time response on the inferred velocity as a possible cause of the large discrepancy between the calculated and inferred coolant flow velocities at the commercial PWR. A model of the coolant transit dynamics was developed to remove the effects of the thermocouple time response on the inferred coolant velocity. The model depicted in Fig. 8 is divided into the transit dynamics $e^{-j\omega\tau}$ and the sensor dynamics $G_s(j\omega)$. The overall transfer function relating neutron flux noise to core exit temperature noise is given by

$$G(j\omega) = e^{-j\omega\tau} G_s(j\omega) \quad . \qquad (11)$$

Solving for the phase of the coolant transit delay:

$$-\omega\tau = \text{phase } [G(j\omega)] - \text{phase } [G_s(j\omega)] \quad . \qquad (12)$$

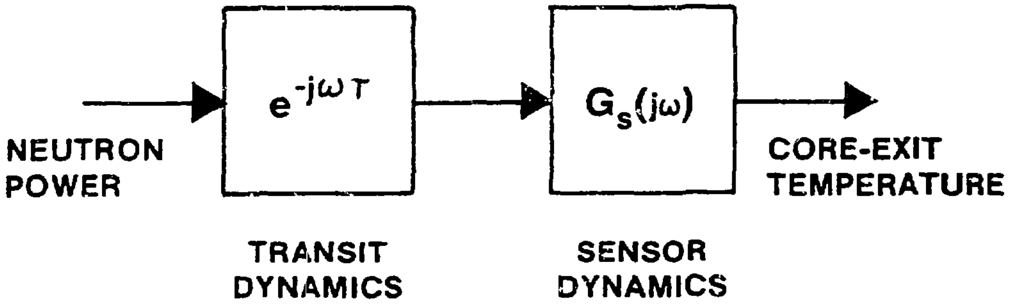

$$G(j\omega) = e^{-j\omega\tau} G_s(j\omega)$$

Fig. 8. Model of transit delay and sensor response dynamics.

The overall transfer function G(jω) was obtained by fitting a 15th-order bivariate auto-regressive (AR) time series model to the ex-core neutron and core exit temperature noise signals, as described in ref. 10. The AR model has the form

$$\underline{Y}(k) = \sum_{i=1}^{n} \underline{\underline{A}}_i \, \underline{X}(k-i) + \underline{V}(k) \quad , \qquad (13)$$

where $\underline{\underline{A}}_i$ are the 2 × 2 parameter matrices, and $\underline{V}$ is a two-element vector of noise sources. The noise vector $\underline{V}$ is assumed to be uncorrelated in time (i.e., "white" noise) with zero mean. Details of parameter estimation and model order selection are given in ref. 10. The bivariate model was transformed to the frequency domain, and the phase of G(jω) was determined.

The sensor dynamics $G_s(j\omega)$ was determined by fitting a 10th-order univariate AR model [i.e., A and V are scalar quantities in Eq. (13)] to the core exit temperature noise signal. The phase angle of $G_s(j\omega)$ (shown in Fig. 9) was subtracted from the phase of G(jω); the resulting phase angle is compared with G(jω) in Fig. 9. With the thermocouple time response effect on the phase between the ex-core ionization chamber and the core exit thermocouple noise removed, the inferred velocity is 4.34 m/s (14.25 ft/s), or ~9% lower than the calculated coolant velocity.

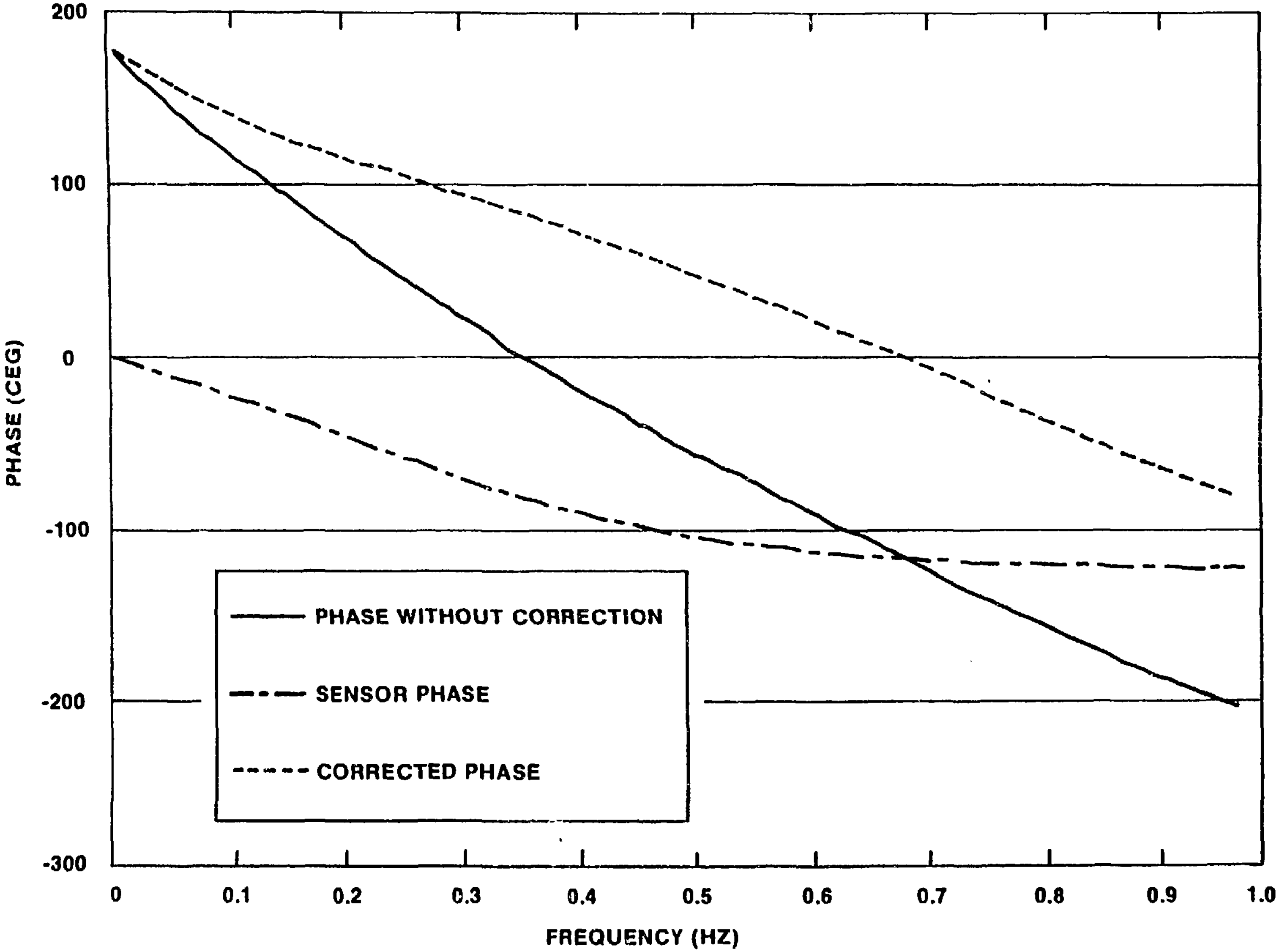

Fig. 9. Comparison of the overall response $G(j\omega)$ and the thermocouple response $G_s(j\omega)$ phase angles with the transit delay $(e^{-j\omega\tau})$ phase angle corrected for the thermocouple time response phase.

A similar procedure was followed with the LOFT data, resulting in a negligible change in the inferred velocities. Thermocouple time constants were obtained from the univariate models of the LOFT and commercial PWR temperature noise by techniques described in ref. 11. A thermocouple time constant of 0.677 s was obtained for the commercial PWR sensor, compared to 0.241 s for the LOFT sensor. We conclude from these results that the large discrepancy between the calculated and inferred velocities obtained from the commercial PWR data is due to the relatively slow thermocouple time response.

CONCLUSIONS

As a result of our work, we believe that temperature noise could play an important part in the surveillance for thermal-hydraulic anomalies in PWRs. The similarity of commercial PWRs with LOFT, and out-of-core test loop temperature noise behavior indicates that these facilities can be used to study the potential application of temperature noise analysis to the detection of anomalies in PWRs during normal operation and for post-accident damage assessments.

In summary:

1. Core exit thermocouple temperature noise RMS increases linearly with increasing core ΔT in PWRs.

2. The RMS temperature noise vs core ΔT curve is not flow dependent over the limited range of flows studied.
3. The time delay between core exit temperature noise and neutron noise is directly related to the coolant flow velocity in the core.
4. If the response time of the temperature sensor is long compared to the coolant transit time between sensors, the inferred flow velocities are lower than measured flow velocities.

REFERENCES

1. D. N. Fry and W. H. Leavell, Temperature Noise Analysis at the Exit of Blocked and Unblocked, 19-Pin Electrically Heated LMFBR Fuel Assembly Mockups, ORNL/TM-5464, Union Carbide Corp., Nuclear Div., Oak Ridge National Laboratory, (1976).
2. E. Turkcan, "Results of the Temperature Noise Measurements in Subchannels of Sodium Cooled Electrically Heated 28 Rod Bundle Behind a Blockage," Prog. Nucl. Energy 1, (1977), 497-506.
3. L. Krebs and G. Weinkotz, "Detection of Local Boiling in an LMFBR Subassembly by Temperature Fluctuation Analysis at the Outlet," Prog. Nucl. Energy 1, (1977), 507-515.
4. T. Tsunoda, "Application of Temperature Fluctuation to Anomaly Detection in Fuel Assemblies," J. Nucl. Sci. Technol. 13, (1976), 103-110.
5. E. Ohlmer and D. Schwalm, "The Use of the Amplitude Distribution of Temperature Noise for Malfunction Detection in a Simulated Reactor Subassembly," Atomkernenergie 25, (1975), 281-284.
6. D. N. Fry, "Application of Noise Analysis to Safety-Related Diagnostics and Assessments," NRC

Seventh Water Reactor Safety Research Information Meeting, National Bureau of Standards, (1979).

7. B. R. Upadhyaya and F. J. Sweeney, "Theoretical and Experimental Analysis of PWR Core Heat Transfer Modeling for In-Core Diagnostics," to appear in Proceedings of the Fifth Power Plant Dynamics, Control, and Testing Symposium, Knoxville, Tennessee, (March 1983).

8. D. N. Fry, Oak Ridge National Laboratory, Oak Ridge, Tennessee, personal communication to F. J. Sweeney, Oak Ridge National Laboratory, Oak Ridge, Tennessee, (1982).

9. T. Katona et al., "Some Aspects of the Theory of Neutron Noise Due to Propogating Disturbances," Third Specialists' Meeting on Reactor Noise (SMORN-III), Tokyo, (1982).

10. B. R. Upadhyaya et al., "Multivariate Signal Analysis Algorithms for Process Monitoring and Parameter Estimation in Nuclear Reactors," Ann. Nucl. Energy 7, (1980), 1-11.

11. B. R. Upadhyaya and T. W. Kerlin, "Estimation of Response Time Characteristics of Platinum Resistance Thermometers by the Noise Analysis Technique," ISA Trans. 17, (1978), 21-38.